



THE EFFECTS OF EXPERIMENTAL CONFIGURATION ON MTDSC FOR SPECIFIC HEAT CAPACITY MEASUREMENTS ACCORDING TO ASTM E 2716-09

*Eveline De Robertis*¹, *Gabriela F. Moreira*², *Rodrigo S. Neves*³, *Carlos E. C. Galhardo*⁴, *Carlos A. Achete*⁵

¹ National Institute of Metrology, Standardization and Industrial Quality (Inmetro), Duque de Caxias-RJ, Brazil, erobertis@inmetro.gov.br

² National Institute of Metrology, Standardization and Industrial Quality (Inmetro), Duque de Caxias-RJ, Brazil, gfmoreira@inmetro.gov.br

³ National Institute of Metrology, Standardization and Industrial Quality (Inmetro), Duque de Caxias-RJ, Brazil, rsneves@inmetro.gov.br

⁴ National Institute of Metrology, Standardization and Industrial Quality (Inmetro), Duque de Caxias-RJ, Brazil, cegalhardo@inmetro.gov.br

⁵ COPPE/UFRJ - Programa de Engenharia Metalúrgica e de Materiais, Rio de Janeiro-RJ, Brazil, achete@metalmat.ufrj.br

Abstract: This work aims at implementing the technique of Modulated Temperature Differential Scanning Calorimetry (MTDSC) to measure the specific heat in various types of samples, according to the standard ASTM E2716. For this, the influence of the experimental parameters was evaluated.

Key words: specific heat capacity, modulated temperature differential scanning calorimetry, experimental configuration, ASTM E 2716-09.

1. INTRODUCTION

Differential scanning calorimetry (DSC) is a thermal analysis technique used for more than thirty years to measure a wide variety of material properties including heat capacity. Most DSC measurements are simple, fast and accurate and require only a single experiment to access thermal behavior and thermophysical properties of materials. However the measurement of heat capacity requires a minimum of three experiments and provided accuracies typically good to only $\pm 10\%$ [1].

Modulated temperature differential scanning calorimetry (MTDSC) is a new technique, introduced in 1992, which provides not only the same information as conventional DSC, but also additional information by overcoming most of the conventional DSC limitations, such as: the lack of possibility to properly analyze simultaneous events, the insufficient sensitivity for events presenting small relaxation times, the absence of adequate resolution and the need of complex experiments.

Both techniques calculate heat capacity from the heat flow resulting from the difference between the sample and one reference. In a DSC and MTDSC experiments this heat flow is described by:

$$dQ/dt = C_p \beta + f(T, t) \quad (1)$$

where dQ/dt is the resultant heat flow, C_p is the heat capacity of the sample, β is the rate of temperature change (dT/dt) and $f(T, t)$ is the heat flow from kinetic processes.

Therefore, it is possible to measure the heat flux in a linear rising temperature experiment and then, calculate heat

capacity by dividing the heat flow by the heating rate and subtracting the kinetic component.

MTDSC differs from conventional DSC in that a low-frequency perturbation ranging from approximately 0.001 to 0.1 Hz is superimposed to the baseline temperature profile. The use of a modulated temperature signal allows the response to multiple frequencies to be measured at one time. And can be expressed as:

$$T = T_0 + \beta t + B \sin \omega t \quad (2)$$

where B is the amplitude of the modulated heating rate and ω is the angular frequency of the modulation.

The derivative of equation 2 with respect to the time is:

$$dT/dt = \beta + \omega B \cos \omega t \quad (3)$$

From heat capacity definition, when the temperature is changing, the heat flow rate required to increase the temperature of a material by 1 degree Kelvin or Celsius is given by:

$$dQ/dt = C_p dT/dt \quad (4)$$

Combining equations 3 and 4, it follows:

$$dQ/dt = C_p (\beta + \omega B \cos \omega t) \quad (5)$$

For the case where β is zero:

$$dQ/dt = C_p \omega B \cos \omega t \quad (6)$$

For the simplest case, from equation 6, the resultant heat flow must be an alternate signal in phase with the sinusoidal temperature perturbation, with amplitude equals to A_{HF} . Therefore:

$$A_{HF} = C_p \omega B \quad (7)$$

From equation 3, it follows that ωB is the amplitude of the modulation in the heating rate, A_{HR} . Thus, C_p can be written as:

$$C_p = A_{HF}/A_{HR} \quad (8)$$

All the signals are calculated from three measured signals: time, modulated temperature and modulated heat flow. The total heat flow in MTDSC experiments is calculated from the average of the heat flow, which corresponds to the total heat flow in a conventional DSC experiment at the same underlying heating rate. Although C_p can be calculated from the difference between two runs on an identical sample at two different heating rates in DSC experiments, in MTDSC it can be determined in a single experiment from the ratio of the modulated heat flow amplitude and the modulated heating rate amplitude by discrete Fourier transformation (equation 8) [2,3]. Experimentally the results are obtained as specific heat capacity, and can be calculated at the temperature of interest from:

$$C_{p_s} = (60s/min \cdot A_{mHF} \cdot K_{C_p}) / (A_{mHR} \cdot W_s) \quad (9)$$

where:

C_{p_s} is the specific heat capacity of the specimen, J/g °C;

A_{mHF} is the amplitude of the modulated heat flow measured at the temperature of interest, mW;

A_{mHR} is the amplitude of the modulated heating rate measured at the temperature of interest, °C/min;

W_s is the mass of the sample, mg;

K_{C_p} is the calibration constant, obtained from the ratio of the theoretical value of sapphire (reference material) to the measured value at the test temperature.

MTDSC signal of total heat flow or apparent specific heat can be split into reversing and non-reversing components. The reversing component of the heat flow is obtained from the amplitude of the first harmonic of the heat flow A_{mHF} , using a Fourier transform of the data. Dividing A_{mHF} by the amplitude of the applied heating rate, A_{mHR} , gives the reversing component of the apparent specific heat:

$$C_{p,rev} = A_{mHF}/W_s A_{mHR} \quad (10)$$

The non-reversing specific heat is the difference between the normalized average heat flow divided by the underlying heating rate β and the reversing specific heat:

$$C_{p,non} = \langle P \rangle / W_s \beta - C_{p,rev} \quad (11)$$

In the absence of other thermal events, the reversing specific heat is simply the frequency-independent heat capacity C_p and the non-reversing specific heat is zero. Initially, the reversing heat flow was considered to reflect only reversible heat effects sensible to changes in the heat capacity, whilst the non-reversing heat flow was considered to reflect primarily irreversible kinetic effects. This assumption is valid only if the kinetics associated with the processes being measured are linear and if the kinetic response does not contribute to the first harmonic [4].

Despite the MTDSC advantages for heat capacity determination, the method is affected by some of the same experimental vicissitudes related to conventional DSC. The difficulty is that many parameters can affect experiments results, therefore it is not an easy task to specify the conditions for reliable measurements. Such parameters are the type of pan used, the carrier gas, the type of the sample (powder, liquid, thin film or chunks) and its physical characteristics (size, shape, thickness, roughness and density).

Considering these parameters, in this work the first aspects investigated were the pan type and sample thickness.

2. EXPERIMENTAL

DSC and MTDSC measurements were carried out on a DSC Q2000 from TA Instruments. The temperature and heat flow signals were calibrated in accordance with Practice E967-08 [5] and E968 [6], respectively, using indium (NIST SRM # 2232). The heat capacity signal for specific heat capacity measurements under modulated temperature conditions was calibrated in accordance with Practice E2716-09 [7], using synthetic sapphire disc reference material. MTDSC runs were recorded in the -60 to 400 °C temperature range using 3 °C/min heating rate, and a sinusoidal temperature perturbation of 1.0 °C amplitude, and 10 mHz frequency.

Metallic copper was chosen for this study. The samples were chunks of electrolytic copper 99.999% purity, cut in several different thickness and copper nanoparticles. The samples were placed in T0 aluminum hermetic pans and aluminum non-hermetic flat pans. For comparison, a theoretic curve of C_p of copper was calculated using Shomate equation and the data available in NIST webbook page [8]:

$$C_p^0 = A + B \cdot t + C \cdot t^2 + D \cdot t^3 + E \cdot t^{-2} \quad (12)$$

where C_p is the heat capacity in J·mol⁻¹·K⁻¹ and t is the temperature in K/1000. For copper $A = 17.72891$, $B = 28.0987$, $C = -31.25289$, $D = 13.97243$ and $E = 0.068611$.

3. RESULTS

All results presented here are averaged from at least four runs with a maximum of nine runs. As a common feature, the experimental specific heat tends to be lower than the calculated one due to cell purge gas since, mainly at higher temperatures, the nitrogen gas thermal conductivity may alter the heat transfer characteristics of the cell. This effect can be minimized using low purge flow rates [9].

The first example of the experimental configuration influence in specific heat values between -50 and 400 °C for copper chunk of 1.000 mm samples is showed in Figure 1.

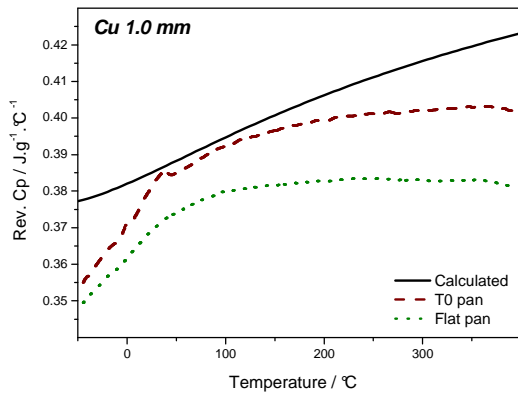


Fig. 1. Specific heat curves of copper chunk samples in two different pans obtained in MTDSC mode under dynamic atmosphere of N_2 (50 mL/min), $3\text{ }^\circ\text{C/min}$ heating rate, $1\text{ }^\circ\text{C}$ amplitude, 100 s period; and specific heat curve calculated for copper using Shomate Equation.

From the comparison between the experimental and calculated curves, some considerations can be done. The curve obtained using T0 pan is more irregular, and considering its volume, which is bigger when compared to the flat aluminum pan, the existence of trapped air inside the pan can explain the raise in specific heat value. However, it is difficult to achieve the reason of these irregularities. This phenomenon can be minimized using a pan which does not provide much space for trapped air.

The influence of sample thickness is exemplified in Figure 2. Although there is no trend directly related to the thickness of the samples, the values of specific heat are close to each other. Substantial deviations in specific heat values are observed for the thinner sample (0.300 mm). These deviations can be explained by the greater presence of air inside the pan. Similarly, as was observed for the sample in T0 pan, above about $120\text{ }^\circ\text{C}$ the curve also presents some small irregularities.

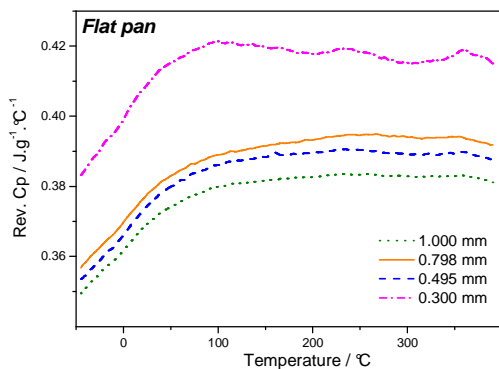


Fig. 2. Specific heat curves of copper samples with different thickness in flat pans obtained in MTDSC mode under dynamic atmosphere of N_2 (50 mL/min), $3\text{ }^\circ\text{C/min}$ heating rate, $1\text{ }^\circ\text{C}$ amplitude, 100 s period.

As pointed out before, an increase in the air amount trapped inside the pan can cause an increase in specific heat values. As can be seen in Figure 3, the experiments performed with the thinner sample resulted in higher specific heat values. In spite of the values of specific heat are closer than the calculated ones, the influence of purge

gas cannot be neglected. Therefore, both effects are difficult to differentiate.

Another way to verify the influence of thermal contact is using copper samples as particles, where discontinuities are introduced because of the shape of the particles. In this case the specific heat values found were shifted to even lower values and the change in the slope of the curve occurred around $20\text{ }^\circ\text{C}$.

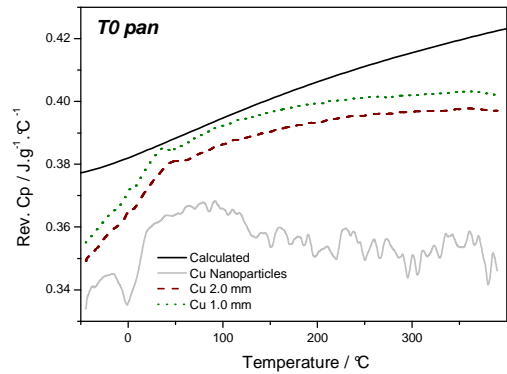


Fig. 3. Specific heat curves of copper samples (chunks and nanoparticles) in T0 pans obtained in MTDSC mode under dynamic atmosphere of N_2 (50 mL/min), $3\text{ }^\circ\text{C/min}$ heating rate, $1\text{ }^\circ\text{C}$ amplitude, 100 s period; and specific heat curve calculated for copper using Shomate Equation.

For nanoparticles sample lower specific heat values are expected due to particle size effect [10] when compared with the calculated values and those obtained from chunk samples. The deviations from linearity observed for this sample can be attributed to poor thermal contact due to particle agglomeration during the separation process, which leads to non uniformities in the overall density.

In Figure 4 an example with its standard deviation is showed. The maximum relative standard deviation is about 2.81%. With the exception of the results of nanoparticles, where the maximum relative standard deviation is about 9.21%, for all the other results the maximum relative standard deviations are lower than 2%.

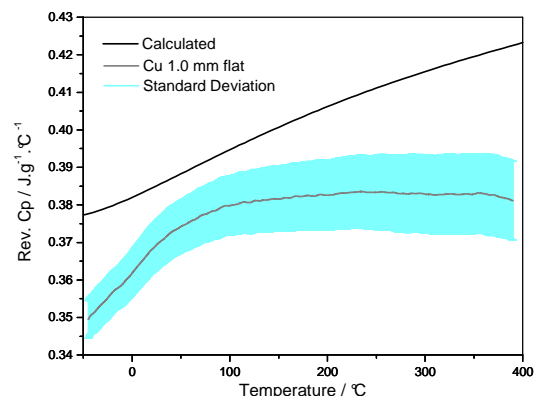


Fig. 4. Specific heat curve and standard deviation of copper sample in flat pan obtained in MTDSC mode under dynamic atmosphere of N_2 (50 mL/min), $3\text{ }^\circ\text{C/min}$ heating rate, $1\text{ }^\circ\text{C}$ amplitude, 100 s period; and specific heat curve calculated for copper using Shomate Equation.

Although there is a tendency of the specific heat increases with temperature, after c.a. 65 °C there is a change in the slope of the curve, which is a characteristic phenomenon for copper. In metals the free electrons make a contribution to specific heat that results in a linear dependence of C on T at low temperatures [11,12].

Above 10 K the lattice vibrations dominate the specific heat. The atoms vibrate near their equilibrium positions and there are no rotational degrees of freedom. Each vibrational degree of freedom involves potential and kinetic energy giving a thermal energy of kT per degree of vibrational freedom. Since there are three independent directions, the average vibrational energy is $3kT$. For N atoms, the internal energy $U=3NkT$ and the specific heat at constant volume is:

$$C_v = \left(\frac{\partial U}{\partial T} \right)_v = 3Nk = 3R \quad (13)$$

Where k is Boltzmann's Constant and R is the Universal Gas Constant.

Since C_v is much more difficult to measure, it is usually obtained from a thermodynamic relation and can be evaluated from the Nernst-Lindemann equation:

$$C_{p_s} - C_v = AC_{p_s}^2 T \quad (14)$$

where the quantity $A = V\beta^* / KC_{p_s}^2$ is found to be nearly temperature independent and V is the molar volume; β^* the volume expansivity and K the isothermal compressibility. For copper it is 3.703×10^{-6} moles/J from 100 to 1200 K [11].

In Figure 5 specific heat at constant volume calculated from equation 14 for two different samples and for the copper C_v curve calculated from Shomate equation (equation 12) are showed together with the value of $3R$ (equation 13). The temperature where the slope of the curves changes is around 65 °C, this temperature is near of the Debye Temperature, θ_D , for copper: 42 °C. θ_D is a measure of the temperature separating the low-temperature region where quantum statistics must be used from the high-temperature where classical statistical mechanics is valid and therefore the sample will behave according to Law of Dulong-Petit described by equation 13 [11,12].

From Figure 5, one can observe that above ca. 65 °C the values of C_v tend to stabilize in a value, this value is 10% below of $3R$.

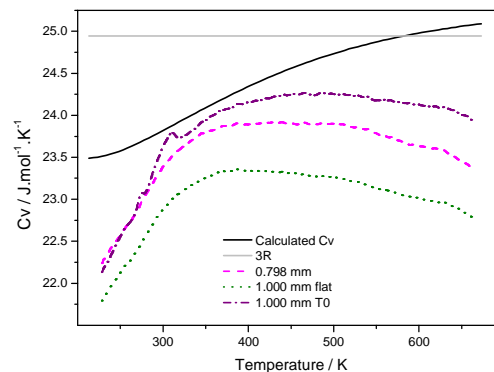


Fig. 5. Specific heat curves at constant volume calculated of copper samples with different thickness in T0 and flat pans obtained in MTDSC mode under dynamic atmosphere of N_2 (50 mL/min), 3 °C/min heating rate, 1 °C amplitude, 100 s period; specific heat curve calculated for copper using Shomate Equation; and 3R constant.

4. CONCLUSION

The evidence of experimental configuration effect (pan type and sample shape) in specific heat measurement is evident. Some of these features can be optimized if not only the experimental configuration but also experimental parameters such as purge gas rate, heating rate, period or amplitude are changed.

Concerning to C_p determination, the MTDSC methodology has good repeatability. However, it should be carefully evaluated, mainly with respect to the influence of different experimental parameters, as the studied here, on the obtained results, in order to get reliable results with satisfactory accuracy and precision

ACKNOWLEDGEMENTS

The authors are grateful to the Brazilian agencies: Financiadora de Estudos e Projetos (FINEP), Fundação de Amparo à Pesquisa do Estado do Rio de Janeiro (FAPERJ) and Conselho Nacional de Desenvolvimento Científico e Tecnológico (CNPq).

REFERENCES

- [1] ASTM E1269-05, "Standard Test Method for Determining Specific Heat Capacity by Differential Scanning Calorimetry", ASTM International, 6 p, 2005.
- [2] E. Verdonk, K. Schaap, L. C. Thomas, "A discussion of the principles and application of Modulated Temperature DSC (MTDSC)", International Journal of Pharmaceutics, Vol 192, pp 3-20, 1999.
- [3] A. A. Lacey, D. M. Price, M. Reading, "Theory and Practice of Modulated Temperature Differential Scanning Calorimetry" in: *Modulated-Temperature Differential Scanning Calorimetry*. M. Reading and D. J. Hourston (Eds.) Netherlands, Springer, 2006.
- [4] S. L. Simon, "Temperature-Modulated Differential Scanning Calorimetry: Theory and Application", *Thermochemica Acta*, Vol 374, pp 55-71, 2001.

- [5] ASTM E967-08, “*Standard Practice for Temperature Calibration of Differential Scanning Calorimeters and Differential Thermal Analyzers*”, ASTM International, 4p, 2008.
- [6] ASTM E968-02(2008), “*Standard Practice for Heat Flow Calibration of Differential Scanning Calorimeters*”, 5 p, 2008.
- [7] ASTM E2716-09, “*Standard Test Method for Determining Specific Heat Capacity by Sinusoidal Modulated Temperature Differential Scanning Calorimetry*”, ASTM International, 4 p, 2009.
- [8] <<http://webbook.nist.gov/cgi/cbook.cgi?ID=C7440508&Units=SI&Mask=2#Thermo-Condensed>> (Copper)
- [9] V. L. Hill, D. Q. M. Craig, L. C. Feely, “*The Effects of Experimental Parameters and Calibration on MTDSC data*”, International Journal of Pharmaceutics, Vol 192, pp 21-32, 1999.
- [10] L-P. Zhou, B-X. Wang, X-F. Peng, X-Z. Du, Y-P. Yang, 2010, “*On the Specific Heat Capacity of CuO Nanofluid*”, Advanced Mechanical Engineering, 2010, Article ID 172085, 2010.
- [11] R. E. Newnham, *Properties of Materials*”, Oxford University Press, 2005.
- [12] N. W. Ashcroft, N. D. Mermin, “*Solid State Physics*”, W. B. Saunders Company, Phyladelphia, 1976.